International Journal of Innovation and Scientific Research
ISSN 2351-8014 Vol. 14 No. 2 Apr. 2015, pp. 259-267

http://www.ijisr.issr-journals.org/

Numerical Solution of MHD Viscous Flow of Micropolar Fluid Over a Shrinking Sheet using SOR Iterative Procedure

Dr. Mohammad Shafique [1-2]

[1]Ex-AP, Department of Mathematics, Gomal University, D I Khan, Pakistan

[2]Current: Private Teaching/Tutoring in Mathematics, Toronto ON, Canada

ABSTRACT: The Magnetohyderodynamic (MHD) viscous flow of micropolar fluid over a shrinking sheet has been solved numerically. The similarity transformations have been used to reduce the highly nonlinear partial differential equations of motion to ordinary differential equations. The resulting equations are then solved by using successive over relaxation (SOR) iterative procedure. The results have been calculated on three different grid sizes to check the accuracy of the results. The results for problem relates to the flows over a shrinking sheet are computed for various values of the flow parameters *M* and *s*, where *M* is the magnetic parameter and *s* is the wall mass transfer parameter. The numerical results for Micropolar fluids are found in good agreement with those of Newtonian fluids.

KEYWORDS: Micropolar Fluids, Shrinking Sheet and SOR Iterative Procedure.

1 INTRODUCTION

The flow problems are being investigated for shrinking surface due to its importance in extrusion processes.. The magnetohyderodynamic (MHD) boundary layer flow of a Second Grade fluid over a shrinking sheet has been studied by Hayat et al [1]. Fang [2] has been examined boundary layer flow over a shrinking sheet with power-law velocity. The MHD boundary layer flow of fluid over a shrinking sheet has been studied by Fang et al [3]. Nadeem et al [4] and Ara et al [5] have been investigated MHD boundary layer flow of fluid over an exponentially permeable shrinking sheet. The steady boundary layer flow and steady two-dimensional flow of a nanofluid past a nonlinearly permeable stretching/ shrinking sheet is numerically studied by Zaimi et al [6, 7].

Kamal and Hussain [8, 9] obtained the numerical results, using SOR method, for the micropolar fluid motion caused by the stretching of a surface in a rotating fluids and inside a stretching channel. Kamal, Ashraf and Syed [10] considered a two dimensional flow of a micropolar fluid driven by injection between two porous disks. while Shafique and Rashid [11] obtained numerical solution of three dimensional micropolar flows due to a stretching flat surface. Shafique et al [12] have been studied the problem numerical solutions of MHD viscous flow of micropolar fluids due to a shrinking sheet numerically by using SOR iterative procedure.

The problem of MHD flow of micropolar fluid over a shrinking sheet has been examined numerically. The electromagnetic effects for micropolar fluids are taken in to account when considering the flows of electroconducting fluids in a magnetic field. The similarity transformations have been used to reduce the highly nonlinear partial differential equations of motion to ordinary differential equations. The resulting equations are then solved by using SOR iterative procedure [13]. The effects of flow parameters namely the magnetic parameter M and the wall mass transfer parameter s have been observed. The results have been obtained for three different cases of the material constants. The results have been compared with the results of Newtonian fluid as obtained and with the previous results where possible.

2 MATHEMATICAL ANALYSIS

The MHD viscous flow of micropolar fluids is assumed to be steady, laminar and incompressible. The fluid flow due to a continuously shrinking sheet in the frame of two dimensional Cartesian coordinate system is considered. The x-axis is taken along the direction of shrinking surface opposite to sheet motion and y-axis is in the direction perpendicular to it. The fluid is electrically conducting in the presence of a magnetic field of strength B_0. The electromagnetic body force is given as $\underline{f} = -\sigma B_0^2(u,0,0)$. The velocity vector is represented as $\underline{V} = V(u,v)$ and the spin velocity vector is $\underline{\omega} = \omega(0,0,\omega_3)$. The body couples are neglected.

The resulting partial differential equations, with the above assumptions, become:

$$\frac{\partial u}{\partial x} + \frac{\partial v}{\partial y} = 0, \tag{1}$$

$$(\mu + \kappa)\left(\frac{\partial^2 u}{\partial x^2} + \frac{\partial^2 u}{\partial y^2}\right) + \kappa\frac{\partial \omega_3}{\partial y} - \frac{\partial \pi}{\partial x} + \underline{J} \times \underline{B} = \rho\left(u\frac{\partial u}{\partial x} + v\frac{\partial u}{\partial y}\right), \tag{2}$$

$$(\mu + \kappa)\left(\frac{\partial^2 v}{\partial x^2} + \frac{\partial^2 v}{\partial y^2}\right) - \kappa\frac{\partial \omega_3}{\partial x} - \frac{\partial \pi}{\partial y} = \rho\left(u\frac{\partial v}{\partial x} + v\frac{\partial v}{\partial y}\right), \tag{3}$$

$$\gamma\left(\frac{\partial^2 \omega_3}{\partial x^2} + \frac{\partial^2 \omega_3}{\partial y^2}\right) + \kappa\left(\frac{\partial v}{\partial x} - \frac{\partial u}{\partial y}\right) - 2\kappa\omega_3 = \rho j\left(u\frac{\partial \omega_3}{\partial x} + v\frac{\partial \omega_3}{\partial y}\right). \tag{4}$$

The velocity components $\underline{V} = V(u,v)$ and the microrotation vector $\underline{\omega} = \omega(0,0,\omega_3)$ can be written as:

$$u = u(x,y), \quad v = v(0,y), \quad \omega_3 = \omega_3(x,y) \text{ and } \underline{J} \times \underline{B} = f_x = -\sigma {B_0}^2 u \tag{4}$$

The boundary conditions are:

$$\begin{cases} u(x) = -U_w, \quad v(x) = v_w(x), \quad \omega_3 = 0, \quad y \to 0, \\ u(x) \to 0, \quad \omega_3 \to 0, \quad y \to \infty. \end{cases} \tag{5}$$

where the sheet shrinking velocity is $U_w = -U_0 x$ and the wall mass transfer is $v_w(x) = -\sqrt{U_0 \nu}\, f(0)$.

We now make the equations of motion dimensionless by using the following similarity transform:

$$u = U_0 x f'(\eta), \quad v = -\sqrt{U_0 \nu}\, f(\eta) \quad \text{and} \quad \omega_3 = \frac{-\sqrt{U_0^3}\, x}{\sqrt{\nu}} L(\eta). \tag{6}$$

where $\eta = y\sqrt{\frac{U_0}{\nu}}$ is a non-dimensional variable.

The equation of continuity (1) is satisfied. The following equation can be determined from equation (3) as:

$$\frac{\partial \pi}{\partial y} = \nu\frac{\partial^2 v}{\partial y^2} - \frac{\kappa}{\rho}\frac{\partial \omega_3}{\partial x} - v\frac{\partial v}{\partial y}$$

The pressure π can be obtained from this equation by integration with respect to η.

The equation (2) and (4) are reduced to a set of non linear ordinary differential equations

$$f''' + ff'' - f'^2 - M^2 f' - C_1 L' = 0, \tag{7}$$

$$L'' + C_2(f'' - 2L) + C_3(fL' - f'L) = 0. \tag{8}$$

Where *M* is the magnetic parameter with $M^2 = \frac{\sigma B^2}{\rho U_0}$ and here C_1, C_2, C_3 are non-dimensional constants in the form

$$C_1 = \frac{\kappa}{\mu + \kappa}, C_2 = \frac{\kappa \upsilon}{\gamma U_0} \text{ and } C_3 = \frac{\rho j \upsilon}{\gamma}.$$

The dimensions of the parameters involved are as follows:

$$[\mu, \kappa] = MT^{-1}L^{-1}, [\gamma] = MLT^{-1}, [j] = L^2, [\rho] = ML^{-3}, [U_0] = T^{-1} \text{and} [\nu] = L^2T^{-1}.$$

The boundary conditions become:

$$\begin{cases} f = s, \quad f' = -1, \quad L = 0, & \text{at} \quad \eta = 0, \\ f' \to 0, \quad L \to 0, & \text{as} \quad \eta \to \infty, \end{cases} \tag{9}$$

where *s* is the wall mass transfer parameter showing the strength of the mass transfer at the sheet.

3 FINITE DIFFERENCE EQUATIONS

The third order non-linear ordinary differential equation (7) and (8) are reduced in order by taking

$$f' = P. \tag{10}$$

We obtain

$$P'' + P'f - P^2 - M^2 P - C_1 L = 0, \tag{11}$$

$$L'' + C_2(P' - 2L) + C_3(fL' - PL) = 0. \tag{12}$$

The boundary conditions (9) become

$$\begin{cases} f = s, \quad P = -1, \quad L = 0, & \text{at} \quad \eta = 0, \\ P \to 0, \quad L \to 0, & \text{as} \quad \eta \to \infty. \end{cases} \tag{13}$$

The equation (11) and (12) are discritized by using central difference approximation at a typical grid point $\eta = \eta_n$ of the interval [0, ∞).The resulting finite difference equation is given below.

$$(2 + hf_n)P_{n+1} + (2 - hf_n)P_{n-1} - C_1 h(L_{n+1} - L_{n-1}) = (4 + 2h^2 M^2 + 2h^2 P_n)P_n, \tag{14}$$

$$(2 + C_3 hf_n)L_{n+1} + (2 - C_3 hf_n)L_{n-1} + C_2 h(P_{n+1} - P_{n-1}) = (4 + 4C_2 h^2 + 2C_3 h^2 P_n)L_n, \tag{15}$$

where h denotes the grid size and the symbols used denote $f_n = f(\eta_n)$ $P_n = P(\eta_n)$. For computational purposes, we replace the interval [0, ∞) by [0, β) where β is sufficiently large.

4 COMPUTATIONAL PROCEDURE

We now solve numerically the first order ordinary differential equation (10) and the finite difference equation (14) and (15) at each interior grid point of the interval. The equation (10) is integrated by the Simpson's (1/3) rule with the formula of Adams-Moulton, whereas the equation (14) and (15) are solved by using SOR iterative procedure subject to the appropriate conditions.

In order to accelerate the speed of convergence of the SOR method, the optimum value of the relaxation parameter ω_{opt} is estimated between 1 and 2. The optimum value of the relaxation parameter for the problem under consideration is 1.5. The SOR iterative procedure is terminated when the following criterion is satisfied:

$$\max_{i=1}^{n} \left| U_i^{n+1} - U_i^{n} \right| < 10^{-6}$$

where *n* denotes the number of iterations and *U* stands for each of *P, f* and *L.* The accuracy of the solution has been checked for step sizes *h*=0.025, 0.0125 and 0.006.

5 DISCUSSION ON NUMERICAL RESULTS

The results of the numerical computation for the problem under consideration are presented here for distinct values of the flow parameters namely s and *M*. The calculations of the results have been carried out on different grid sizes namely *h*=0.025, 0.0125, 0.006. The calculations have also been made for three sets of material constants C_1, C_2 and C_3 given in the table below.

Case	C_1	C_2	C_3
I	0.1	1.5	1.1
II	0.2	3.0	1.5
III	0.3	0.5	0.2

If the above constants are zero, the micropolar fluids flow becomes the Newtonian fluids flow. The three different cases for the values of the constants have been considered for this micropolar fluids flow problem during the computational work. When C_1 is small and C_2, C_3 are large, the micropolar fluids flow resembles with Newtonian fluids flow as in Case-I. The cases II and III are far from the results of Newtonian fluids due to fast miro rotation of the molecules because of large values of material constants.

Tables 1 to 6 show the comparison of the values for the functions f, f' and *L* in the case-I of the material constants for each of grid sizes. The excellent comparison of the results validates our computational procedure. The comparison of the values of $f''(0)$ for micropolar fluids and Newtonian fluids is given in Table 7.

Graphically, the behavior of f' and *f* has been depicted in Figure 1 to Figure 6. Figure 1 and Figure 2 demonstrate f' and *f* respectively for *M*=1 and positive values of s. The graphs of f' and f have been plotted for *M* =2 and presented in Figure 3 and Figure 4 respectively. When *M* =4, the results of these functions are shown in Figure 5 and Figure 6.

It is noticed that the effect of *M* is stronger for its larger values. The wall shear stress increases with increase in the values of s for all fixed values of *M*. It can be easily observed that initially *f* decreases slightly and then become uniform.

6 CONCLUSION

The effects of different parameters are observed on the similarity, velocity, micro rotation profiles. The wall shear stress increases with increase in the values of s for all fixed values of *M*. It can be easily observed that initially *f* decreases slightly and then become uniform. The function f' increases with the increasing values of s at a fixed value of *M*. The boundary layer becomes thinner for larger s. The increasing values of s increase the micro rotation. The comparison of Micropolar results is excellent with the results Newtonian and reported by Fang et al [3].

Table 1. The results of functions f, f', L in the case-I and for flow parameters M, s

h	η	M=1.0 & s= 0.1			M=1.0 & s=2.0		
		f	f'	L	f	f'	L
0.025	0.000	0.100000	-1.000000	0.000000	2.000000	-1.000000	0.000000
	1.000	-0.858970	-0.918928	0.021512	1.568095	-0.134295	0.042931
	2.000	-1.739811	-0.843681	0.033470	1.510688	-0.017341	0.022220
	3.000	-2.547844	-0.772731	0.040329	1.503502	-0.001973	0.008951
	4.000	-3.281658	-0.686204	0.042801	1.502772	-0.000127	0.002881
	5.000	-3.781522	0.000000	0.000000	1.502747	0.000000	0.000000
0.0125	0.000	0.100000	-1.000000	0.000000	2.000000	-1.000000	0.000000
	1.000	-0.859093	-0.919062	0.020901	1.568233	-0.134175	0.027609
	2.000	-1.739894	-0.843414	0.027134	1.510830	-0.017440	0.007741
	3.000	-2.547409	-0.771990	0.027345	1.503511	-0.002107	0.001248
	4.000	-3.280374	-0.685313	0.030177	1.502674	-0.000205	0.000148
	5.000	-3.779514	0.000000	0.000000	1.502607	0.000000	0.000000
0.006	0.000	0.100000	-1.000000	0.000000	2.000000	-1.000000	0.000000
	1.000	-0.859123	-0.919059	0.024760	1.568242	-0.134162	0.010471
	2.000	-1.739926	-0.843345	0.024937	1.510808	-0.017482	0.000553
	3.000	-2.547219	-0.771711	0.006804	1.503458	-0.002129	0.000037
	4.000	-3.279892	-0.684937	0.003783	1.502607	-0.000212	0.000004
	5.000	-3.778624	0.000000	0.000000	1.502536	0.000000	0.000000

Table 2. The results of functions f, f', L in the case-I and for flow parameters M, s

h	η	M=1.0 & s= 5.0			M=2.0 & s=-6.0		
		f	f'	L	f	f'	L
0.025	0.000	5.000000	-1.000000	0.000000	-6.000000	-1.000000	0.000000
	1.000	4.801831	-0.006462	0.009753	-6.800227	-0.629003	0.027557
	2.000	4.800614	-0.000008	0.001298	-7.303545	-0.395598	0.040321
	3.000	4.800620	0.000004	0.000142	-7.620075	-0.248761	0.044507
	4.000	4.800620	0.000000	0.000014	-7.819076	-0.156316	0.041070
	5.000	4.800620	0.000000	0.000000	-7.932308	0.000000	0.000000
0.0125	0.000	5.000000	-1.000000	0.000000	-6.000000	-1.000000	0.000000
	1.000	4.801687	-0.006525	0.004165	-6.800283	-0.629096	0.032760
	2.000	4.800434	-0.000024	0.000147	-7.303653	-0.395559	0.038988
	3.000	4.800432	0.000002	0.000003	-7.620010	-0.248473	0.024697
	4.000	4.800432	0.000000	0.000000	-7.818689	-0.156014	0.011852
	5.000	4.800432	0.000000	0.000000	-7.931770	0.000000	0.000000
0.006	0.000	5.000000	-1.000000	0.000000	-6.000000	-1.000000	0.000000
	1.000	4.801647	-0.006552	0.000663	-6.800351	-0.629117	0.036279
	2.000	4.800381	-0.000027	0.000002	-7.303646	-0.395465	0.017983
	3.000	4.800379	0.000001	0.000000	-7.619922	-0.248365	0.003067
	4.000	4.800379	0.000000	0.000000	-7.818454	-0.155838	0.001031
	5.000	4.800379	0.000000	0.000000	-7.931354	0.000000	0.000000

Table 3. The results of functions f, f', L in the case-I and for flow parameters M, s

h	η	M=2.0 & s= -4.0			M=1.0 & s=-1.0		
		f	f'	L	*f*	f'	L
0.025	0.000	-4.000000	-1.000000	0.000000	-1.000000	-1.000000	0.000000
	1.000	-4.737042	-0.524761	0.038867	-1.559466	-0.272207	0.051700
	2.000	-5.123742	-0.275254	0.050216	-1.711516	-0.073743	0.044463
	3.000	-5.326523	-0.144280	0.048717	-1.752557	-0.019751	0.028959
	4.000	-5.432733	-0.075394	0.038506	-1.763425	-0.005059	0.015085
	5.000	-5.481737	0.000000	0.000000	-1.765770	0.000000	0.000000
0.0125	0.000	-4.000000	-1.000000	0.000000	-1.000000	-1.000000	0.000000
	1.000	-4.737109	-0.524848	0.042825	-1.559414	-0.272058	0.043730
	2.000	-5.123789	-0.275075	0.041068	-1.711252	-0.073524	0.022988
	3.000	-5.326255	-0.143887	0.021056	-1.752167	-0.019736	0.006333
	4.000	-5.432118	-0.075153	0.008277	-1.763111	-0.005205	0.001295
	5.000	-5.481070	0.000000	0.000000	-1.765598	0.000000	0.000000
0.006	0.000	-4.000000	-1.000000	0.000000	-1.000000	-1.000000	0.000000
	1.000	-4.737164	-0.524797	0.040238	-1.559436	-0.272012	0.024652
	2.000	-5.123745	-0.275040	0.012878	-1.711268	-0.073558	0.002163
	3.000	-5.326185	-0.143807	0.001532	-1.752203	-0.019734	0.000129
	4.000	-5.431950	-0.075053	0.000521	-1.763145	-0.005207	0.000032
	5.000	-5.480806	0.000000	0.000000	-1.765633	0.000000	0.000000

Table 4. The results of functions f, f', L in the case-I and for flow parameters M, s

h	η	M=2.0 & s= 1.0			M=2.0 & s=2.0		
		f	f'	L	*f*	f'	L
0.025	0.000	1.000000	-1.000000	0.000000	2.000000	-1.000000	0.000000
	1.000	0.609069	-0.099751	0.037869	1.683378	-0.049423	0.027532
	2.000	0.570339	-0.009646	0.018848	1.667929	-0.002253	0.009722
	3.000	0.566701	-0.000812	0.007379	1.667284	-0.000048	0.002752
	4.000	0.566438	-0.000021	0.002420	1.667289	0.000015	0.000667
	5.000	0.566444	0.000000	0.000000	1.667297	0.000000	0.000000
0.0125	0.000	1.000000	-1.000000	0.000000	2.000000	-1.000000	0.000000
	1.000	0.609169	-0.099651	0.024366	1.683428	-0.049408	0.015148
	2.000	0.570457	-0.009698	0.005759	1.667940	-0.002315	0.002044
	3.000	0.566745	-0.000887	0.000689	1.667246	-0.000081	0.000135
	4.000	0.566424	-0.000061	0.000055	1.667230	0.000004	0.000005
	5.000	0.566406	0.000000	0.000000	1.667232	0.000000	0.000000
0.006	0.000	1.000000	-1.000000	0.000000	2.000000	-1.000000	0.000000
	1.000	0.609173	-0.099646	0.008037	1.683429	-0.049428	0.003786
	2.000	0.570437	-0.009726	0.000254	1.667915	-0.002332	0.000066
	3.000	0.566708	-0.000896	0.000013	1.667211	-0.000085	0.000002
	4.000	0.566381	-0.000065	0.000001	1.667192	0.000003	0.000000
	5.000	0.566361	0.000000	0.000000	1.667192	0.000000	0.000000

Table 5. The results of functions f, f', L in the case-I and for flow parameters M, s

h	η	M=2.0 & s= 4.0			M=4.0 & s=-6.0		
		f	f'	L	*f*	f'	L
0.025	0.000	4.000000	-1.000000	0.000000	-6.000000	-1.000000	0.000000
	1.000	3.787124	-0.009351	0.012141	-6.447936	-0.149845	0.029902
	2.000	3.785204	-0.000045	0.001984	-6.514992	-0.022362	0.019056
	3.000	3.785205	0.000006	0.000259	-6.524959	-0.003285	0.008332
	4.000	3.785207	0.000001	0.000029	-6.526404	-0.000461	0.002883
	5.000	3.785207	0.000000	0.000000	-6.526594	0.000000	0.000000
0.0125	0.000	4.000000	-1.000000	0.000000	-6.000000	-1.000000	0.000000
	1.000	3.787052	-0.009401	0.005081	-6.447893	-0.149769	0.023870
	2.000	3.785094	-0.000066	0.000206	-6.514896	-0.022350	0.005975
	3.000	3.785084	0.000002	0.000004	-6.524876	-0.003313	0.000504
	4.000	3.785084	0.000000	0.000000	-6.526349	-0.000483	0.000030
	5.000	3.785084	0.000000	0.000000	-6.526552	0.000000	0.000000
0.006	0.000	4.000000	-1.000000	0.000000	-6.000000	-1.000000	0.000000
	1.000	3.787023	-0.009426	0.000752	-6.447907	-0.149768	0.007173
	2.000	3.785054	-0.000069	0.000003	-6.514920	-0.022359	0.000116
	3.000	3.785044	0.000002	0.000000	-6.524900	-0.003303	0.000010
	4.000	3.785044	0.000000	0.000000	-6.526371	-0.000482	0.000002
	5.000	3.785044	0.000000	0.000000	-6.526574	0.000000	0.000000

Table 6. The results of functions f, f', L in the case-I and for flow parameters M, s

h	η	M=4.0 & s= -3.0			M=4.0 & s=1.0		
		f	f'	L	*f*	f'	L
0.025	0.000	-3.000000	-1.000000	0.000000	3.000000	-1.000000	0.000000
	1.000	-3.350530	-0.070454	0.026784	2.823789	-0.003425	0.008020
	2.000	-3.375148	-0.004875	0.011568	2.823210	0.000000	0.000872
	3.000	-3.376820	-0.000305	0.003468	2.823213	0.000001	0.000065
	4.000	-3.376914	-0.000010	0.000821	2.823213	0.000000	0.000004
	5.000	-3.376916	0.000000	0.000000	2.823213	0.000000	0.000000
0.0125	0.000	-3.000000	-1.000000	0.000000	3.000000	-1.000000	0.000000
	1.000	-3.350445	-0.070377	0.017012	2.823782	-0.003449	0.002513
	2.000	-3.375046	-0.004902	0.002365	2.823186	-0.000007	0.000035
	3.000	-3.376748	-0.000331	0.000123	2.823186	0.000000	0.000000
	4.000	-3.376860	-0.000019	0.000004	2.823186	0.000000	0.000000
	5.000	-3.376865	0.000000	0.000000	2.823186	0.000000	0.000000
0.006	0.000	-3.000000	-1.000000	0.000000	3.000000	-1.000000	0.000000
	1.000	-3.350446	-0.070382	0.003606	2.823763	-0.003459	0.000173
	2.000	-3.375058	-0.004910	0.000045	2.823163	-0.000008	0.000000
	3.000	-3.376764	-0.000332	0.000002	2.823163	0.000000	0.000000
	4.000	-3.376877	-0.000020	0.000000	2.823163	0.000000	0.000000
	5.000	-3.376882	0.000000	0.000000	2.823163	0.000000	0.000000

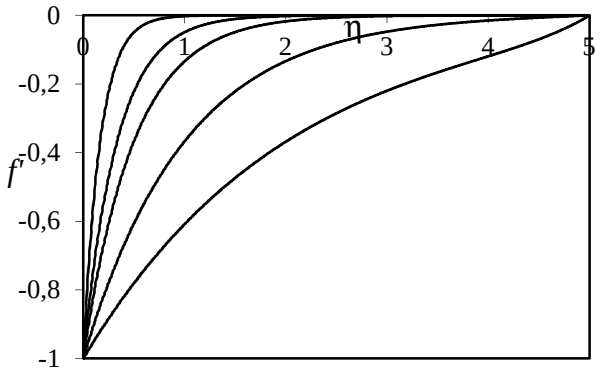

Figure 1: Graph of f' for M=1 and s=0.5,1,2,3 and 6 from top.

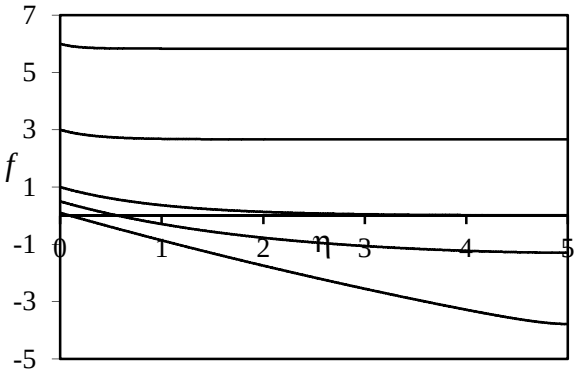

Figure 2: Graph of f for M=1 and different values of s

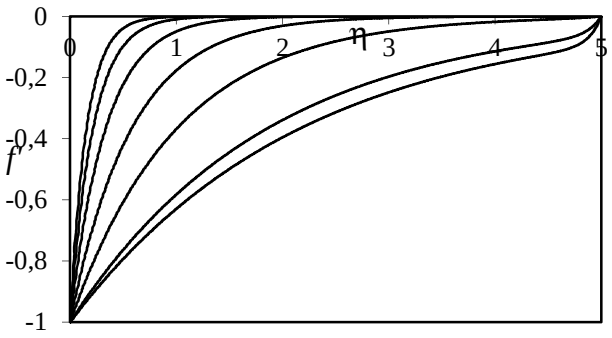

Figure3: Graph of f' for M=2 and different values of s=-6,-5,-2,0,2,4 and 6 from top.

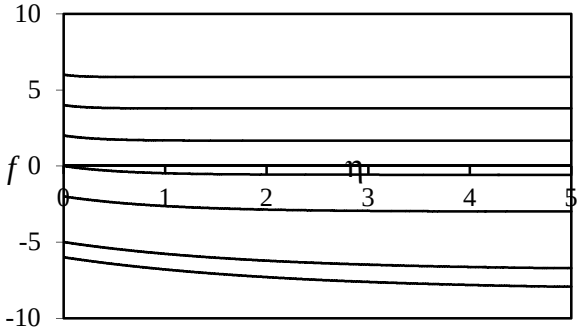

Figure4: Graph of f for M=2 and different values of s

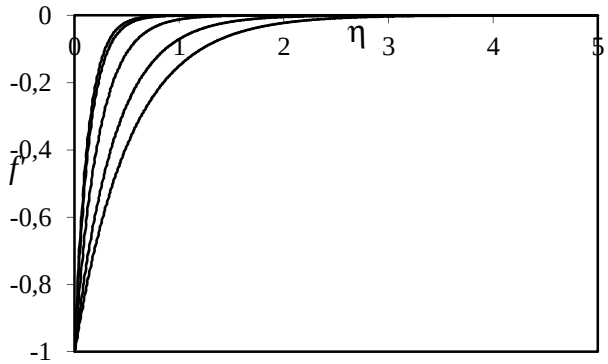

Figure5: Graph of f' for M=4 and different values of s=-6,-3,1,3 and 6 from top.

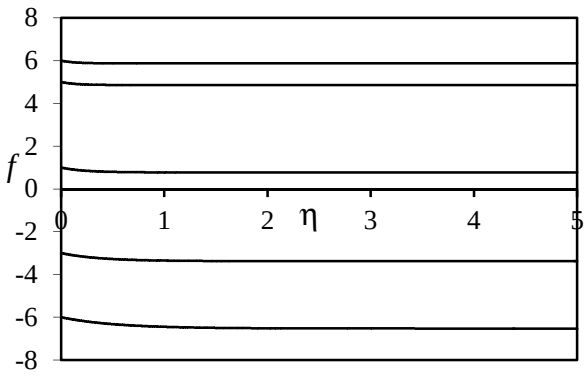

Figure6: Graph of f for M=4 and different values of s

Table 7: The comparison of Micropolar fluids and Newtonian fluids for $f''(0)$

M	s	Micropolar fluids			Newtonian fluids	
		I	II	III	Present Results	Previous Results [3]
1	1.0	0.991964	0.933962	0.862684	0.996923	1.00000
	3.0	2.972517	2.992992	2.934408	2.971773	3.00000
	5.0	4.923592	4.914522	4.908409	4.923077	5.00000
	6.0	5.890122	5.923519	5.882006	5.889731	6.00000
2	-5.0	0.539112	0.500002	0.474472	0.540485	0.541381
	-4.0	0.642527	0.5907822	0.549173	0.644388	0.645751
	-2.0	0.993424	0.909405	0.823355	0.996809	1.00000
	-1.0	1.293154	1.194324	1.0727977	1.297235	1.302775
4	-6.0	1.885499	1.826984	1.772413	1.887569	1.898979
	-5.0	2.094440	2.026815	1.959486	2.095728	2.1097722
	-3.0	2.628965	2.547340	2.449760	2.631159	2.6533119
	-1.0	3.366156	3.280859	3.153353	3.368683	3.4051248
	0.0	3.824530	3.739739	3.606482	3.826008	3.8729833
	1.0	4.343233	4.248524	4.131737	4.344549	4.4051248
	3.0	5.553141	5.472822	5.392885	5.554104	5.653311
	5.0	6.953611	6.908465	6.822863	6.954012	7.109772
	6.0	7.707100	7.674437	7.599907	7.706906	7.898979

REFERENCES

[1] T. Hayat, Z. Abbas and M. Sajid, (2007), On the Analytic Solution of MHD Flow of a Second Grade Fluid Over a Shrinking Sheet, .J. Appl. Mech. 74(6), 1165-1171

[2] Tiegang Fang, (2008), Boundary layer flow over a shrinking sheet with power-law velocity, International Journal of Heat and Mass Transfer, Volume 51, Issues 25–26, 5838–5843.

[3] Fang, T. and Zhang, Ji. (2009), Closed- Form exact solutins of MHD viscous flow over a shrinking sheet, Commun Nonlinear Sci Numer Sumulat, 14, 2853 –2857.

[4] S. Nadeem, Rizwan Ul Haq, C. Lee, (2012), MHD flow of a Casson fluid over an exponentially shrinking sheet,Scientia Iranica B 19 (6), 1550–1553.

[5] Asmat Ara, Najeeb Alam Khan, Hassam Khan, Faqiha Sultan, (2014), Radiation effect on boundary layer flow of an Eyring–Powell fluid over an exponentially shrinking sheet, Ain Shams Engineering Journal, Volume 5, Issue 4, 1337–1342.

[6] Khairy Zaimi, Anuar Ishak & Ioan Pop, (2014), Boundary layer flow and heat transfer over a nonlinearly permeable stretching/shrinking sheet in a nanofluid, Scientific Reports4, Article number:4404 doi:10.1038/ srep04404.

[7] Khairy Zaimi,, Anuar Ishak, Ioan Pop , (2014), Flow Past a Permeable Stretching/Shrinking Sheet in a Nanofluid Using Two-Phase Model, PLoS ONE 9(11): e111743.

[8] M.A. Kamal and S. Hussain. Stretching of a surface in a rotating micropolar fluid, Int. J. Sci. Tech., spring-fall,30-36,(1994).

[9] M.A. Kamal and S. Hussain. (1994). Steady flow of a micropolar fluid in a channel with an accelerating surface velocity, Journal of Natural Sciences and Mathematics, 34(1), 23-40.

[10] M.A. Kamal, M. Ashraf, and K. S. Syed. (2006), Numerical solution of steady viscous flow of a micropolar fluid driven by injection between two porous disks. App Math. & Comp, 179(1), 1-10.

[11] M. Shafique and A. Rashid (2006), Numerical study of the three dimensional micropolar flows due to a stretching flat surfaceint. J. of Matheematics and Analysis, 1(2),175-189.

[12] M. Shafique , Fatima Abbas, A Rashid. MHD Viscous Flow of Micropolar Fluids due to a Shrinking Sheet. International Journal of Emerging Technology and Advanced Engineering, Volume 3, Issue 7, 651-658, 2013.

[13] C. F. Gerald, "Applied Numerical Analysis," Addison- Wesley Publication, New York, 1989.